Finite Deflection Discrete Element Analysis of Sandwich Plates and Cylindrical Shells with Laminated Faces

L. A. Schmit Jr.* and G. R. Monforton†
Case Western Reserve University, Cleveland, Ohio

A discrete element analysis capability for predicting the geometrically nonlinear behavior of sandwich plate and cylindrical shell structures with unbalanced laminated faces is reported. The geometric admissibility conditions of the principle of minimum total potential energy are conveniently satisfied by employing bicubic Hermite interpolation polynomials to approximate the displacement behavior. Specialization for the finite deflection analysis of thin anisotropic and transversely heterogeneous plate and cylindrical shell systems is achieved by simply considering one face of the sandwich. Numerical solutions are obtained by direct minimization of the total potential energy using a scaled conjugate gradient algorithm. Several problems are solved which illustrate the potential of the method for predicting the finite deflection and elastic postbuckling behavior of sandwich and thin laminated structures.

Introduction

An increasing number of structural designs, especially in the aerospace industry, are utilizing laminated and sandwich-type construction in the fabrication of major structural components. Also, composite materials have been developed and design methods and concepts are evolving in order to make efficient use of these new materials. The inherent low-stiffness characteristics of glass-reinforced plastics, for example, often limits their effective use to sandwich construction. However, the field of filamentary composites is developing from one dealing primarily with glass-reinforced plastics to a much broader class including boron, graphite, and metal fibers. The substantial interest in these new high-strength and low-density materials in both solid laminate and sandwich construction is evidence of the continual quest for strong lightweight structures.

Unbalanced laminated construction (i.e., a section where the lamina are placed unsymmetrically, elastically, and/or geometrically about the middle surface) is characterized by coupling between extensional and flexural action. This type of behavior warrants a greater emphasis on anisotropic and transversely heterogeneous (i.e., nonhomogeneous through the thickness) shell analyses. Furthermore, the desire for minimum weight optimum structural designs has resulted in the development and application of structural synthesis techniques for the design of load carrying systems. Naturally, the use of these new design optimization methods tends to undercut the validity of employing analysis methods which are based on the usual linearizing assumptions of structural analysis. In order to balance the analysis and design methods, it becomes more realistic to base the equilibrium equations on the deformed geometry, to employ more exact deformation-displacement relations, and to consider the nonlinear behavior of the material.

Presented at the 10th AIAA/ASME Structures, Structural Dynamics and Materials Conference, New Orleans, La., April 14–16 (no page number; published in bound volume of conference papers); submitted December 15, 1969; revision received March 11, 1970. Sponsored by the Advanced Research Projects Agency, Department of Defense through Contract AF 33(615)-3110, administered by the Air Force Materials Laboratory, Wright-Patterson Air Force Base, Ohio.

* Wilbert J. Austin Professor of Engineering; presently Professor of Engineering, University of California, Los Angeles, Calif.

† Graduate Assistant; presently Assistant Professor, Civil Engineering Department, University of Windsor, Windsor, Ontario, Canada.

For lightweight structures, such as the sandwich and thin laminated shell structures often encountered in aerospace design practice, situations involving geometric nonlinearities (including general instability) but restricted to linear elastic anisotropic material behavior constitute an interesting and significant class of analysis problems. This is especially true in the case of sandwich systems where the range of deflections for which small deflection theory is valid decreases as the shear stiffness of the core is made small compared to that of the faces.[1]

It has been found that geometric nonlinearities can be conveniently dealt with using a discrete element method based on the principle of minimum total potential energy. The development presented herein follows the approach of Refs. 2–4 which begins with the selection of nonlinear strain-displacement equations. This is followed by the adoption of a strain energy density potential function consistent with the linear stress-strain law to be represented. The potential energy for the discrete element is then obtained by integrating the strain energy density over the element volume and adding the potential of the external loads applied to the element. The selection of the assumed displacement patterns for the element is a crucial step and consideration must be given to the geometric admissibility requirements, completeness, and rigid body displacement states.[4] Substitution of the assumed displacement functions into the potential energy expression for the element leads to the discretized form of the element potential energy.

This paper reports on a finite deflection discrete element analysis capability for sandwich plates and cylindrical shells with unbalanced laminated faces. A segment of a sandwich cylindrical shell is shown in Fig. 1. The radius of the middle surface of the core is denoted by R_c and its thickness is t_c. Arbitrary reference surfaces in the skins are located at distances d_f from the interfaces between the core and skins ($f = 1, 2$ where the subscript 1 refers to the lower or inner face and the subscript 2 refers to the upper or outer face). The radii of the skin reference surfaces are denoted R_f and the face thicknesses are t_f. The coordinate system and displacement components are also shown in Fig. 1.

The faces of the sandwich system are considered to behave as thin shells and may be composed of an arbitrary number of bonded layers, each of which may have different thickness, linear elastic anisotropic material properties, and orientation of elastic axes. The orthotropic core is considered to be relatively thick and typical of that used in honeycomb sandwich construction. It is assumed that the transverse deflection is finite and uniform through the thickness of the sandwich system. It is also assumed that the rotations of the deformed structure relative to the undeformed position are small and that bond failure at the interfaces between the core and skins does not occur. Under these conditions the strain energy of the sandwich system is a collection of the following: 1) quadratic strain energy terms in the displacement variables due to membrane action of the faces in their reference planes; 2) quadratic, cubic, and quartic strain energy contributions, due to bending in the faces; 3) quadratic and cubic strain energy terms due to coupling between membrane and bending action in the faces; and 4) quadratic strain energy terms due to transverse shearing in the core. The strain energies due to transverse shearing of the faces and due to face-parallel deformations in the core are considered negligible.

Formulation

Based on the usual thin shell theory assumptions (including the Kirchhoff-Love conditions), the nonlinear strain-displacement relations for the unbalanced laminated faces of a sandwich cylinder can be represented by

$$\epsilon_{fx} = \epsilon^{\circ}{}_{fx} + z_f\kappa_{fx},\ \epsilon_{fy} = \epsilon^{\circ}{}_{fy} + z_f\kappa_{fy},\ \gamma_{fxy} = \gamma^{\circ}{}_{fxy} + z_f\kappa_{fxy} \qquad (1)$$

where z_f is measured from the reference surface and the reference surface strains are defined by

$$\epsilon^{\circ}{}_{fx} = u_{fx} + \tfrac{1}{2}w_{fx}{}^2,\ \epsilon^{\circ}{}_{fy} = v_{fy} + (1/R_f)w_f + \tfrac{1}{2}w_{fy}{}^2$$
$$\gamma^{\circ}{}_{fxy} = v_{fx} + u_{fy} + w_{fx}w_{fy} \qquad (2)$$

The curvature expressions are defined by

$$\kappa_{fx} = -w_{fxx},\ \kappa_{fy} = -w_{fyy} + (1/R_f)v_{fy}$$
$$\kappa_{fxy} = -2[w_{fxy} - (1/R_f)v_{fx}] \qquad (3)$$

In the preceding expressions the notation

$$u_{fx} = \frac{\partial u_f}{\partial x},\ u_{fy} = \frac{\partial u_f}{\partial y_f} = \frac{1}{R_f}\frac{\partial u_f}{\partial \theta},\ \text{etc. } (f = 1,2)$$

has been adopted for convenience. The corresponding nonlinear strain-displacement equations for the faces of sandwich plates are obtained directly from Eq. (1) by setting $y_f = y$ and $1/R_f = 0$.

The force-deformation equations for the faces can be expressed as[5]

$$\begin{Bmatrix} N_{fx} \\ N_{fy} \\ N_{fxy} = N_{fyx} \\ \hline M_{fx} \\ M_{fy} \\ M_{fxy} = M_{fyx} \end{Bmatrix} = \left[\begin{array}{ccc|ccc} A_{f11} & A_{f12} & A_{f16} & B_{f11} & B_{f12} & B_{f16} \\ & A_{f22} & A_{f26} & B_{f12} & B_{f22} & B_{f26} \\ & & A_{f66} & B_{f16} & B_{f26} & B_{f66} \\ \hline & & & D_{f11} & D_{f12} & D_{f16} \\ & (\text{Symmetric}) & & & D_{f22} & D_{f26} \\ & & & & & D_{f66} \end{array}\right] \begin{Bmatrix} \epsilon^{\circ}{}_{fx} \\ \epsilon^{\circ}{}_{fy} \\ \gamma^{\circ}{}_{fxy} \\ \hline \kappa_{fx} \\ \kappa_{fy} \\ \kappa_{fxy} \end{Bmatrix} \qquad (4)$$

where N_{fx}, N_{fy}, $N_{fxy} = N_{fyx}$ are the force resultants, M_{fx}, M_{fy}, $M_{fxy} = M_{fyx}$ are the moment resultants and the A_{fij}, B_{fij}, D_{fij} (f = 1, 2; i, j = 1, 2, 6) represent the membrane, coupling, and bending stiffnesses of the faces. Note that nonzero values of the coupling stiffnesses B_{fij} are characteristic of unbalanced laminated construction and indicate that coupling between membrane and bending action exists even for the small deflection theory of such flat plates; the B_{fij} are zero when the lamina are placed symmetrically about the middle surface and when the reference surface coincides with the middle surface. Various methods are available for determining the A_{fij}, B_{fij}, and D_{fij}; the discussions that follow are based on the premise that they can be obtained by theoretical, empirical, or experimental methods. In this way the formulation presented herein is independent of the method used to obtain the stiffnesses.

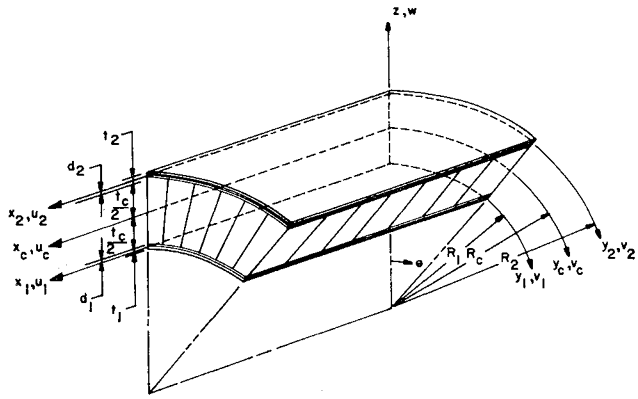

Fig. 1 Laminated sandwich cylindrical shell segment.

The strain energy of a face can be expressed as

$$U_f = U_{f2} + U_{f3} + U_{f4} \qquad (5)$$

where U_{f2}, U_{f3}, and U_{f4} represent the contributions to the strain energy which appear as quadratic, cubic, and quartic terms, respectively, in the displacement variables u_f, v_f, and w_f. For the unbalanced laminated faces under consideration U_{f2}, U_{f3}, and U_{f4} are given below:

$$\begin{aligned} U_{f2} = \frac{1}{2}\int_{S_f} \Bigg\{ & [A_{f11}u_{fx}{}^2 + A_{f22}v_{fy}{}^2 + A_{f66}(u_{fy} + v_{fx})^2 + 2A_{f12}u_{fx}v_{fy} + 2A_{f16}(u_{fy} + v_{fx})u_{fx} + 2A_{f26}(u_{fy} + v_{fx})v_{fy}] - {} \\ & 2[B_{f11}u_{fx}w_{fxx} + B_{f22}v_{fy}w_{fyy} + 2B_{f66}(u_{fy} + v_{fx})w_{fxy} + B_{f12}(v_{fy}w_{fxx} + u_{fx}w_{fyy}) + B_{f16}(u_{fy} + v_{fx})w_{fxx} + {} \\ & 2B_{f16}u_{fx}w_{fxy} + B_{f26}(u_{fy} + v_{fx})w_{fyy} + 2B_{f26}v_{fy}w_{fxy}] + [D_{f11}w_{fxx}{}^2 + D_{f22}w_{fyy}{}^2 + 4D_{f66}w_{fxy}{}^2 + 2D_{f12}w_{fxx}w_{fyy} + {} \\ & 4D_{f16}w_{fxx}w_{fxy} + 4D_{f26}w_{fyy}w_{fxy}] + \frac{1}{R_f}\Bigg[\frac{A_{f22}}{R_f}w_f{}^2 + 2\left(A_{f22} + \frac{B_{f22}}{R_f}\right)w_fv_{fy} + \left(\frac{D_{f22}}{R_f} + 2B_{f22}\right)v_{fy}{}^2 - {} \\ & 2B_{f22}w_fw_{fyy} - 2D_{f22}v_{fy}w_{fyy} + 4\left(\frac{D_{f66}}{R_f} + B_{f66}\right)v_{fx}{}^2 + 4B_{f66}v_{fx}u_{fy} - 8D_{f66}v_{fx}w_{fxy} + 2A_{f12}w_fu_{fx} - 2B_{f12}w_fw_{fxx} + {} \\ & 2B_{f12}u_{fx}v_{fy} - 2D_{f12}v_{fy}w_{fxx} + 4B_{f16}u_{fx}v_{fx} - 4D_{f16}v_{fx}w_{fxx} + 2A_{f26}w_fu_{fy} - 4B_{f26}w_fw_{fxy} + 2\left(A_{f26} + 2\frac{B_{f26}}{R_f}\right)w_fv_{fx} + {} \\ & 2B_{f26}u_{fy}v_{fy} - 4D_{f26}v_{fy}w_{fxy} + 2\left(2\frac{D_{f26}}{R_f} + 3B_{f26}\right)v_{fx}v_{fy} - 4D_{f26}v_{fx}w_{fyy}\Bigg]\Bigg\}\, dS_f \end{aligned} \qquad (6)$$

$$\begin{aligned} U_{f3} = \frac{1}{2}\int_{S_f} \Bigg\{ & [A_{f11}u_{fx}w_{fx}{}^2 + A_{f22}v_{fy}w_{fy}{}^2 + 2A_{f66}(u_{fy} + v_{fx})w_{fx}w_{fy} + A_{f12}(u_{fx}w_{fy}{}^2 + v_{fy}w_{fx}{}^2) + A_{f16}(u_{fy} + {} \\ & v_{fx})w_{fx}{}^2 + 2A_{f16}u_{fx}w_{fx}w_{fy} + A_{f26}(u_{fy} + v_{fx})w_{fy}{}^2 + 2A_{f26}v_{fy}w_{fx}w_{fy}] - [B_{f11}w_{fxx}w_{fx}{}^2 + B_{f22}w_{fyy}w_{fy}{}^2 + {} \\ & 4B_{f66}w_{fx}w_{fy}w_{fxy} + B_{f12}(w_{fxx}w_{fy}{}^2 + w_{fyy}w_{fx}{}^2) + 2B_{f16}(w_{fxy}w_{fx}{}^2 + w_{fx}w_{fy}w_{fxx}) + 2B_{f26}(w_{fxy}w_{fy}{}^2 + {} \\ & w_{fx}w_{fy}w_{fyy})] + \frac{1}{R_f}[A_{f22}w_fw_{fy}{}^2 + A_{f12}w_fw_{fx}{}^2 + 2A_{f26}w_fw_{fx}w_{fy} + B_{f22}v_{fy}w_{fy}{}^2 + 4B_{f66}v_{fx}w_{fx}w_{fy} + {} \\ & B_{f12}v_{fy}w_{fx}{}^2 + 2B_{f16}v_{fx}w_{fx}{}^2 + 2B_{f26}v_{fy}w_{fx}w_{fy} + 2B_{f26}v_{fx}w_{fy}{}^2]\Bigg\}\, dS_f \end{aligned} \qquad (7)$$

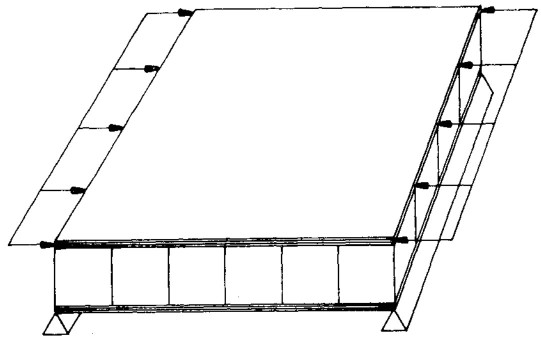

Fig. 2 **Sandwich plate with mixed boundary conditions.**

$$U_{f4} = \tfrac{1}{2} \int_{S_f} \{\tfrac{1}{4}[A_{f11}w_{fx}{}^4 + A_{f22}w_{fy}{}^4] + [A_{f66} + \tfrac{1}{2}A_{f12}]w_{fx}{}^2 w_{fy}{}^2 + [A_{f16}w_{fx}{}^3 w_{fy} + A_{f26}w_{fx}w_{fy}{}^3]\} dS_f \quad (8)$$

In the preceding expressions, S_f is the reference surface area of the faces. Also, the strain energy for the faces of sandwich plates can be extracted from Eqs. (6–8) by setting $y_f = y$ and $1/R_f = 0$.

The filler which separates the faces is orthotropic, relatively thick, and representative of honeycomb sandwich cores. It it assumed that the core is incompressible in the transverse direction, that the face-parallel shear and extensional stiffnesses are negligible, and that the face-parallel displacements vary linearly through the thickness of the core.

The strain-displacement equations for the core of a sandwich cylinder can be represented by

$$\gamma_{cxz} = w_{cx} + \phi_c,\ \gamma_{cyz} = [1/(1 + z_c/R_c)] \times [w_{cy} - (1/R_c)v_{cx} + \psi_c] \quad (9)$$

where z_c is measured from the middle surface and ϕ_c and ψ_c are rotations of normals to the middle surface. Again the notation

$$w_{cx} = \frac{\partial w_c}{\partial x};\ w_{cy} = \frac{\partial w_c}{\partial y_c} = \frac{1}{R_c}\frac{\partial w_c}{\partial \theta} \text{ etc.}$$

has been adopted for convenience. It is assumed that bond failure does not occur at the interfaces between the filler and skins and that the transverse displacement is constant through the thickness of the sandwich. Using these conditions, the core shear strain-displacement equations, Eqs. (9), can be expressed in terms of the membrane displacements of the individual faces and the transverse displacements of the sandwich;

$$\gamma_{cxz} = \gamma^\circ{}_{cxz} = \frac{1}{t_c}[u_2 - u_1 + (d_1 + d_2 + t_c)w_x]$$

$$\gamma_{cyz} = \gamma^\circ{}_{cyz} \bigg/ \left(1 + \frac{z_c}{R_c}\right) = \frac{1}{t_c}[e_2 v_2 - e_1 v_1 + e_3 w_{cy}] \bigg/ \left(1 + \frac{z_c}{R_c}\right) \quad (10)$$

where

$$e_1 = 1 + (t_c/2R_c),\ e_2 = 1 - (t_c/2R_c)$$

$$e_3 = d_1\left(\frac{R_c}{R_1} + \frac{t_c}{2R_1}\right) + d_2\left(\frac{R_c}{R_2} - \frac{t_c}{2R_2}\right) + t_c \quad (11)$$

The corresponding strain-displacement equations for the core of a sandwich plate are obtained by setting $y_c = y$, $R_c/R_1 = R_c/R_2 = 1$ and $1/R_1 = 1/R_2 = 1/R_c = 0$.

The force-deformation equations for the core can be expressed as

$$\begin{Bmatrix} Q_{cyz} \\ Q_{cxz} \end{Bmatrix} = \begin{bmatrix} B_{44} & 0 \\ 0 & B_{55} \end{bmatrix} \begin{Bmatrix} \gamma^\circ{}_{cyz} \\ \gamma^\circ{}_{cxz} \end{Bmatrix} \quad (12)$$

where Q_{cxz} and Q_{cyz} are the transverse shear force resultants. The B_{44} and B_{55} are the transverse shear stiffnesses of the core and can be obtained by theoretical or experimental methods.

It is assumed that the strain energy contribution of the core is due to transverse shear only and it can therefore be expressed as

$$U_c = \frac{1}{2}\int_{S_c}\left\{\frac{B_{44}}{t_c^2}[e_2 v_2 - e_1 v_1 + e_3 w_{cy}]^2 + \frac{B_{55}}{t_c^2}[u_2 - u_1 + (d_1 + d_2 + t_c)w_x]^2\right\} dS_c \quad (13)$$

where S_c is the middle surface area of the core.

The potential of the applied loads is restricted to the work done by loads applied to the individual faces. The work done by these applied loads is represented by

$$W_f = \int_{S_f} [\bar{p}_{fx}u_f + \bar{p}_{fy}v_f + \bar{p}_{fz}w_f]dS_f + \oint_{y_f}\left[\bar{N}_{fx}u_f + \bar{N}_{fxy}v_f + \bar{Q}_{fxz}w_f - \bar{M}_{fx}w_{fx} - \bar{M}_{fxy}\left(w_{fy} - \frac{v_f}{R_f}\right)\right]dy_f - \oint_x\left[\bar{N}_{fyx}u_f + \bar{N}_{fy}v_f + \bar{Q}_{fyz}w_f - \bar{M}_{fyx}w_{fx} - \bar{M}_{fy}\left(w_{fy} - \frac{v_f}{R_f}\right)\right]dx \quad (14)$$

The terms $\bar{p}_{fx}$, $\bar{p}_{fy}$, $\bar{p}_{fz}$ denote tractions applied to the reference surfaces in the x, y_f, and z directions, respectively. The forces ($\bar{N}_{fx}$, $\bar{N}_{fy}$, $\bar{Q}_{fxz}$, $\bar{Q}_{fyz}$, $\bar{N}_{fxy}$, $\bar{N}_{fyx}$) and moments ($\bar{M}_{fx}$, $\bar{M}_{fy}$, $\bar{M}_{fxy}$, $\bar{M}_{fyx}$) are the components of the applied forces and moments acting on the edges of the faces.

The total potential energy π_p of the sandwich system is the sum of the potential energy of the two faces and the core

$$\pi_p(u_1,u_2,v_1,v_2,w) = U_c + \sum_{f=1}^{2}(U_f - W_f) \quad (15)$$

Note that in the formulation presented, the potential energy is expressed in terms of the four membrane displacements of

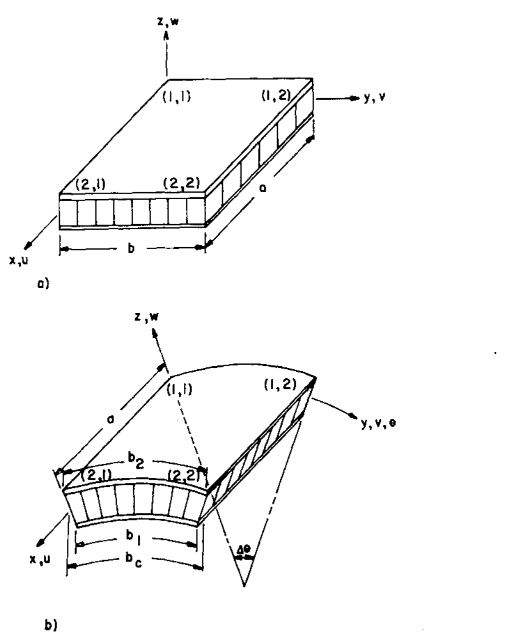

Fig. 3 Anisotropic sandwich elements: a) sandwich plate element; b) sandwich cylindrical shell element.

the faces (u_1,u_2,v_1,v_2) and the transverse displacement of the sandwich system (w). This choice of displacement variables admits transverse shear deformations in the core and allows a rather wide range in the choice of boundary conditions. For example, it is possible to impose membrane displacement boundary conditions on one face while allowing the other face to satisfy natural or imposed force boundary conditions (Fig. 2). Furthermore, this choice of displacement variables is such that the finite displacement analysis of thin unbalanced laminated plates and cylindrical shells is a special case obtained by simply considering one face of the sandwich.

Discretization

The sandwich plate and cylindrical shell elements are shown in Fig. 3. The displacement variables u_1, u_2, v_1, v_2, and w are represented by assumed displacement functions which can readily satisfy the geometric admissibility conditions of the principle of minimum total potential energy. The displacement functions used herein are of the form suggested in Ref. 6 and have been successfully employed to predict the geometric nonlinear behavior of thin isotropic plate and cylindrical shell systems.[3] The displacement patterns are formed in terms of products of one-dimensional first-order Hermite interpolation polynomials (bicubic) and undetermined nodal coefficients. For example, the longitudinal displacement of a face in the sandwich cylindrical shell element can be represented as

$$u_f(x,y_f) = \sum_{i=1}^{2}\sum_{j=1}^{2} [H_{oi}^{(1)}(x)H_{oj}^{(1)}(y_f)u_{fij} + H_{1i}^{(1)}(x)H_{oj}^{(1)}(y_f)u_{fxij} + H_{oi}^{(1)}(x)H_{1j}^{(1)}(y_f)u_{fyij} + H_{1i}^{(1)}(x)H_{1j}^{(1)}(y_f)u_{fxyij} \quad (16)$$

where the particular values of the indices i and j refer to the node (i,j) of the element. The $H_{ki}^{(1)}$ are the first-order Hermite interpolation polynomials given by

$$\begin{aligned} H_{oi}^{(1)}(x) &= (2x^3 - 3ax^2 + a^3)/a^3 \\ H_{o2}^{(1)}(x) &= -(2x^3 - 3ax^2)/a^3 \\ H_{11}^{(1)}(x) &= (x^3 - 2ax^2 + a^2x)/a^2 \\ H_{12}^{(1)}(x) &= (x^3 - ax^2)/a^2 \end{aligned} \quad (17)$$

Similar expressions for the circumferential direction are obtained by replacing x by y_f and a by b_f where the subscript f indicates that distances are measured along the appropriate reference surfaces. The nodal coefficients u_{fij}, u_{fxij}, u_{fyij}, u_{fxyij} are directly related to the displacement and derivatives of the displacement at the nodal points. For example, $u_{fij} = u_f(x = x_i, y_f = y_{fj} \equiv R_f\theta_j)$, and $u_{fyij} = \partial u_f/\partial y_f(x = x_i, y_f = y_{fj} \equiv R_f\theta_j) = 1/R_f \partial u_f/\partial\theta(x = x_i, \theta = \theta_j)$.

Expressions similar to Eq. (16) are used for the remaining displacement variables ($v_f, f = 1,2$, and w). The bicubic interpolation polynomials used in the formulation of these sandwich elements were selected for the following reasons. 1) They readily permit satisfaction of the geometric admissibility conditions for both sandwich or thin plate and cylindrical shell systems. 2) They give an accurate representation of the elemental strain energy for both rigid body and deformation inducing displacements. 3) They provide the capability of imposing strain continuity of the reference surfaces. (For typical sandwich systems where the bending stiffnesses of the faces are small, imposing strain continuity results in accurate stress predictions that are especially important in predicting the postbuckling behavior of a structural system.) 4) They provide the capability to model structures using elements joined at arbitrary angles.

Substituting the assumed displacement patterns into the strain energy expressions for the two faces and the core [Eqs. (6–8, and 13)] and performing the indicated integrations over the appropriate reference surfaces yields the total discretized strain energy for the sandwich plate or cylindrical shell element expressed compactly as

$$U = U_c + \sum_{f=1}^{2} U_f = \frac{1}{2}\bar{X}^T K_2 \bar{X} + \frac{1}{2}\bar{X}^T K_3 \bar{Y} + \frac{1}{2}\bar{Y}^T K_4 \bar{Y} \quad (18)$$

The vector $\bar{X}$ contains the eighty undetermined nodal coefficients of the element (16 associated with each of u_1, u_2, v_1, v_2, w). The vector $\bar{X}$ can be partitioned as

$$\underset{(1\times 80)}{\bar{X}^T} = \{\bar{U}_1{}^T,\bar{U}_2{}^T,\bar{V}_1{}^T,\bar{V}_2{}^T,\bar{W}^T\} \quad (19)$$

where, for example

$$\underset{(1\times 16)}{\bar{U}_1{}^T} = \{u_{111},u_{1x11},u_{1y11},u_{1xy11},u_{112},u_{1x12},u_{1y12},u_{1xy12}, u_{122},u_{1x22},u_{1y22},u_{1xy22},u_{121},u_{1x21},u_{1y21},u_{1xy21}\} \quad (20)$$

Similar definitions are made for $\bar{U}_2$, $\bar{V}_1$, $\bar{V}_2$, and $\bar{W}$. The vector $\bar{Y}$ contains the 136 possible quadratic combinations of the 16 degrees of freedom associated with w. The usual stiffness matrix associated with quadratic portion of the strain energy, K_2, can be partitioned as

$$\underset{(80\times 80)}{K_2} = \begin{bmatrix} K_2^{(u_1u_1)} & K_2^{(u_1u_2)} & K_2^{(u_1v_1)} & 0 & K_2^{(u_1w)} \\ & K_2^{(u_2u_2)} & 0 & K_2^{(u_2v_2)} & K_2^{(u_2w)} \\ & & K_2^{(v_1v_1)} & K_2^{(v_1v_2)} & K_2^{(v_1w)} \\ & \text{(symmetric)} & & K_2^{(v_2v_2)} & K_2^{(v_2w)} \\ & & & & K_2^{(ww)} \end{bmatrix} \quad (21)$$

All the submatrices in K_2 are 16 × 16 arrays; those on the diagonal are symmetric and contain contributions that do not involve coupling between the various displacement components. Generally the off-diagonal arrays are not symmetric and account for the coupling terms in the quadratic portion of the strain energy; the superscripts indicate which displacements are coupled. Explicit formulas for the elements of the submatrices in K_2 are given in Ref. 7. The matrix K_3 in Eq. (18) is associated with the cubic terms in the strain energy and contains terms which couple u_f, v_f, $(f = 1,2)$ and w; K_3 can be partitioned as

$$\underset{(80\times 136)}{K_3} = \begin{bmatrix} K_3^{(u_1w)} \\ K_3^{(u_2w)} \\ K_3^{(v_1w)} \\ K_3^{(v_2w)} \\ K_3^{(ww)} \end{bmatrix} \quad (22)$$

Each of the submatrices in K_3 is a 16 × 136 rectangular array and the superscripts denote coupling between the indicated displacement variables. It is noted that in the absence of face coupling stiffnesses (i.e., if $B_{fij} = 0$) $K_3^{(ww)} = 0$ for flat sandwich and thin plate elements. The matrix $\underset{(136\times 136)}{K_4}$ is associated with the fourth-order strain energy terms which contain contributions involving only the transverse displacement variable.

The discretized work term can be written as

$$W = \bar{X}^T\bar{P} \quad (23)$$

where $\bar{P}$ is a vector containing the 80 work equivalent loads associated with the 80 nodal degrees of freedom residing in the displacement vector $\bar{X}$.

The potential energy of the kth element can be represented by

$$\pi_p^{(k)} = U^{(k)} - W^{(k)} \quad (24)$$

where $U^{(k)}$ and $W^{(k)}$ are given as Eqs. (18) and (23). The total potential energy of an assemblage of N elements can be

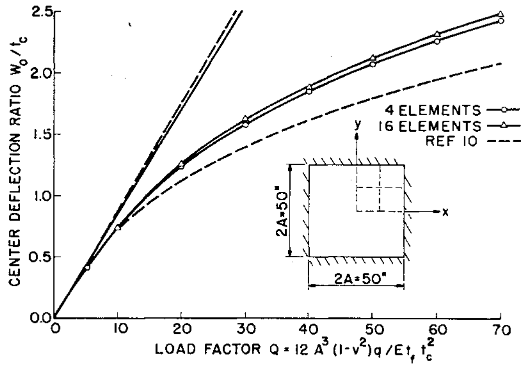

Fig. 4 Clamped sandwich plate.

written as

$$\Pi_p = \sum_{k=1}^{N} \pi_p^{(k)} \tag{25}$$

Implementation and Numerical Examples

The potential energy for an assemblage of elements representing a structural system must be expressed in terms of a set of independent degrees of freedom by satisfying the geometric admissibility conditions prior to seeking an approximate solution. Additional conditions, such as requiring the membrane strains of the faces to be continuous across adjacent edges of sandwich elements, can also be accommodated by the appropriate linking of degrees of freedom. The mechanics of satisfying the necessary and additional conditions for thin shell systems has been thoroughly dealt with in Refs. 3 and 4. Since the procedure is basically the same for the elements considered herein, the reader is referred to Refs. 3 and 4 for the details which lead to the desired set of independent degrees of freedom.

In this work, displacement solutions for structural systems which include the effects of geometrically nonlinear behavior are obtained by a direct search for the local minimum of the total potential energy (note that this statement recognizes the possible existence of relative minima in nonlinear problems and points out the fact that only stable solutions can be found by minimization of the total potential energy). For problems involving many independent degrees of freedom, such as those often encountered in discrete element formulations, the conjugate gradient method of Ref. 8 is appealing since it requires a minimum of matrix manipulations and computer storage. Although the method has been plagued by convergence difficulties, incorporation of the special scaling transformation proposed in Ref. 9 has dramatically improved the convergence characteristics of the method. For the problems dealt within this study, the scaled conjugate gradient algorithm was adopted and found to be effective.

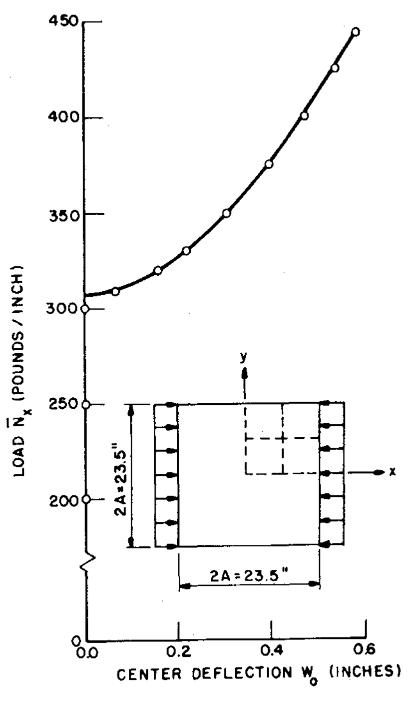

Fig. 5 Compressed sandwich plate.

Several numerical examples have been worked out in order to illustrate the potential of the discrete element capability reported for the prediction of finite displacements and post-buckling behavior of unbalanced laminated and sandwich systems. It is important to note that all the numerical examples presented have the following common characteristics. 1) The geometric admissibility conditions are satisfied ab initio by appropriately linking and/or cancelling degrees of freedom. 2) The reference surface strains of the faces are made continuous by linking certain degrees of freedom between elements. 3) The reference surfaces of the skins are taken to coincide with the skin middle surfaces. Correspondingly the face stiffnesses presented are based on calculations which take $d_f = \frac{1}{2}t_f$ ($f = 1, 2$).

Clamped Sandwich Plate under Uniform Pressure (Fig. 4)

A 50-in. × 50-in. sandwich plate consists of two identical aluminum facings ($E = 10.5 \times 10^6$ psi, $\nu = 0.3$) which are 0.015 in. thick and an aluminum honeycomb core ($G_{cxz} = G_{cyz} = 50{,}000$ psi) which is 1 in. thick. The corresponding stiffnesses for the faces ($f = 1,2$) are

$$A_{f11} = A_{f22} = 1.7308 \times 10^5 \text{ lb/in.};\quad A_{f12} = 0.5192 \times 10^5 \text{ lb/in.}$$

$$A_{f16} = A_{f26} = 0;\ A_{f66} = 0.6058 \times 10^5 \text{ lb/in.}$$

$$B_{fij} = 0,\ (i,j = 1,2,6)$$

$$D_{f11} = D_{f22} = 3.245 \text{ in.-lb};\ D_{f12} = 0.9736 \text{ in.-lb}$$

$$D_{f16} = D_{f26} = 0;\ D_{f66} = 1.1358 \text{ in.-lb}$$

For the core,

$$B_{44} = B_{55} = 5.0 \times 10^4 \text{ lb/in.}$$

The boundaries of the square sandwich plate are fully clamped so that the imposed displacement boundary conditions are

$$u_1 = u_2 = v_1 = v_2 = w = w_x = 0;\ x = \pm A$$

$$u_1 = u_2 = v_1 = v_2 = w = w_y = 0;\ y = \pm A$$

The system is subjected to a uniform transverse load of q psi. Because of the loading and boundary conditions the behavior is such that $u_1 = -u_2$ and $v_1 = -v_2$. Also the behavior is symmetric about the lines $x = 0$ and $y = 0$ so that only one quadrant of the system is modeled. The sandwich plate was discretized using 4 and 16 elements (41 and 177 degrees of freedom, respectively) and the displacement response was obtained for various values of the pressure load. A curve of center deflection (w_o) vs load parameter $Q = [12A^3(1 - \nu^2)/t_f E_f t_c^2]q$ is plotted in Fig. 4 and comparison is made with the results obtained in Ref. 10. Inspection of Fig. 4 reveals that the nonlinear discrete element solutions are somewhat more flexible than those reported in Ref. 10. The solutions of Ref. 10 were obtained by a method of successive approximations which assumes that the magnitude of the center deflection w_o is of the same order as the core thickness; solutions are then approximated in terms of a perturbation parameter $W_o = w_o/t_c \leq 1$. It is emphasized that the solutions presented in Ref. 10 are limited by a two-term expansion of the dimensionless loading as a function of W_o; the resulting expression for the square sandwich plate was recorded as

$$Q = 11.4074(w_o/t_c) + 5.2596(w_o/t_c)^3$$

It is reasonable to expect that the accuracy of the preceding solution is limited and that more terms would be required, especially when (w_o/t_c) increases much beyond unity.

On the other hand, the 4 and 16 element discrete element solutions for w_o are in very close agreement, indicating that the transverse displacement results can be obtained with relatively coarse modeling. The linear solutions for the 4 and 16 element modelings also agree very closely (e.g., $w_o = 1.71$ in. for 16 elements and $w_o = 1.70$ in. for 4 elements at $Q = 20$). These are plotted as one solid line in Fig. 4, and compared with the linear successive approximation solution ($w_o = 1.75$ in. at $Q = 20$).

Compressed Sandwich Plate (Fig. 5)

Consider a square 23.5-in. × 23.5-in. simply supported sandwich plate with identical isotropic facings ($t_1 = t_2 = 0.021$ in.; $E = 9.5 \times 10^6$ psi, $\nu = 0.3$) and a 0.181-in. thick core ($G_{cxz} = G_{cyz} = 1.9 \times 10^4$ psi). The membrane and bending stiffnesses of the faces are ($f = 1, 2$)

$$A_{f11} = A_{f22} = 2.1923 \times 10^5 \text{ lb/in.}; \; A_{f12} = 0.6577 \times 10^5 \text{ lb/in.}$$

$$A_{f16} = A_{f26} = 0; \; A_{f66} = 0.7673 \times 10^5 \text{ lb/in.}$$

$$B_{fij} = 0, \; (i,j = 1,2,6)$$

$$D_{f11} = D_{f22} = 8.0567 \text{ in.-lb}; \; D_{f12} = 2.4170 \text{ in.-lb}$$

$$D_{f16} = D_{f26} = 0; \; D_{f66} = 2.8200 \text{ in.-lb}$$

and the transverse shear stiffnesses of the core are $B_{44} = B_{55} = 3.439 \times 10^3$ lb/in. Assuming a symmetrical buckling pattern one quadrant of the plate was modeled using 4 nonlinear sandwich plate elements. In accordance with general practice it was assumed that transverse shear strains are prevented along the core boundaries. The imposed displacement boundary conditions are represented by

$$w = 0, \; v_1 = v_2 \text{ at } x = \pm A$$

$$w = 0; \; u_1 = u_2 \text{ at } y = \pm A$$

The plate was subjected to inplane loads $\bar{N}_{1x} = \bar{N}_{2x} = \frac{1}{2}\bar{N}_x$ lb/in. along the edges $x = \pm A$. Linking appropriate degrees of freedom to insure geometric admissibility and requiring membrane strain continuity, the problem is reduced to the minimization of a function of 106 variables.

The load $\bar{N}_x$ vs center deflection w_o is plotted in Fig. 5. The critical load predicted by the minimization of the total discretized potential energy is obtained from the intersection of the load-deflection curve with the load axis. The buckling load is found to be $\bar{N}_{CR} = 307.5$ lb/in. as compared to a value of 308 lb/in. reported in Ref. 11.

The plot of Fig. 5 indicates that the plate remains flat until the critical load is attained. With an increase in load into the postbuckled region, the center deflection increases but the system becomes stiffer. It is noted that the solutions were obtained by first applying a transverse load to the system and obtaining the solution corresponding to this loading. This perturbed solution was then used as a starting point in the search for the minimum of the potential energy under the load $\bar{N}_x = 440$ lb/in.; this energy search produced the postbuckled displacement state for $\bar{N}_x = 440$ lb/in. and subsequent points on the load deflection curve were obtained by decreasing $\bar{N}_x$ until only linear flat solutions could be obtained.

Compressed Orthotropic Composite Thin Plate (Fig. 6)

A thin (0.055-in.) plate is constructed by bonding four orthotropic graphite fiber reinforced plies (0°, 90°, 90°, 0°) such that the laminated plate has a balanced configuration. The plate is equivalent to an orthotropic plate with the following membrane and bending stiffnesses:

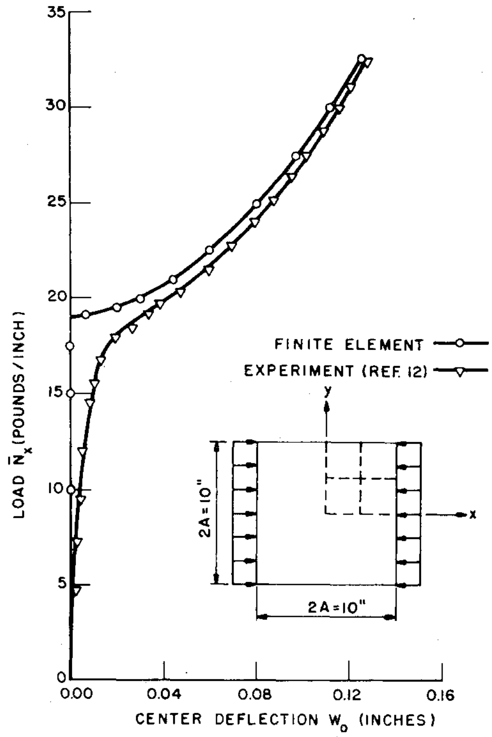

Fig. 6 Compressed orthotropic plate.

$$A_{11} = 3.118 \times 10^5 \text{ lb/in.}; \; A_{12} = 1.768 \times 10^4 \text{ lb/in.}$$

$$A_{22} = 3.118 \times 10^5 \text{ lb/in.}; \; A_{16} = A_{26} = 0$$

$$A_{66} = 2.730 \times 10^4 \text{ lb/in.}$$

$$D_{11} = 127.0 \text{ in.-lb}; \; D_{12} = 4.45 \text{ in.-lb}$$

$$D_{22} = 30.2 \text{ in.-lb}; \; D_{16} = D_{26} = 0; \; D_{66} = 6.88 \text{ in.-lb}$$

$$B_{ij} = 0 \; (i,j = 1,2,6)$$

The 10-in. × 10-in. plate is simply supported on all four sides and is subjected to compressive load, $\bar{N}_x$ lb/in. along the edges $x = \pm 5.0$ in. Taking symmetry into account one quadrant of the plate was modeled using four 2.5-in. × 2.5-in. nonlinear elements (only the lower face of the sandwich plate element was considered). A curve of the center deflection w_o vs the applied load $\bar{N}_x$ was plotted in Fig. 6. A load deflection curve for the plate was obtained from experimental studies in Ref. 12 (plate 201), and this experimental plot is also shown in Fig. 6. Comparison of the two curves indicates the postbuckling behavior predicted by the nonlinear discrete element method is in excellent agreement with the test results. The slight discrepancy between the two curves can be attributed to the usual discretization and experimental errors as well as to initial imperfections in the test panel; the experimental curve is typical of load-deflection curves for structures with initial imperfections exhibiting a stable-symmetric postbuckling behavior.[13]

The buckling load predicted by the present method is $N_{CR} = 19.2$ lb/in. The "exact" results according to classical orthotropic plate theory is $N_{CR} = 19.1$ lb/in. (Ref. 14) whereas a Southwell plot of the experimental results of Ref. 12 indicates a buckling load of $N_{CR} = 21.7$ lb/in.

Compressed Thin Unbalanced Composite Plate (Fig. 7)

A thin (0.109-in.) unbalanced composite plate is considered. The plate is constructed from 20 orthotropic boron reinforced plies; the fibers in the lower 10 plies make an angle

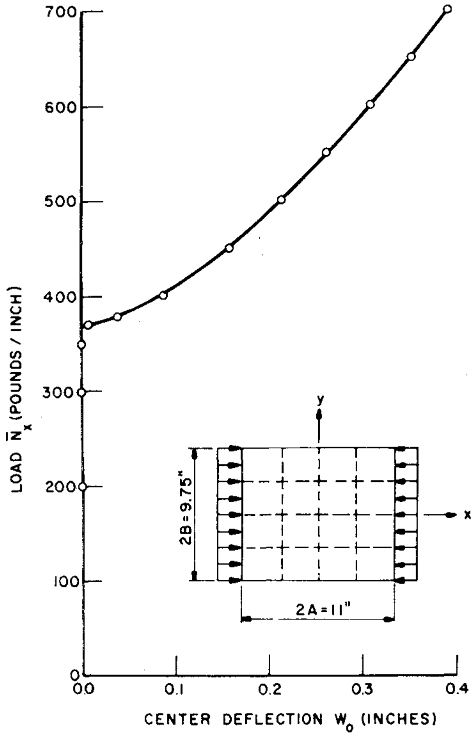

Fig. 7 Compressed unbalanced plate.

of $+45°$ with the x axis of the plate while the fibers in the upper 10 plies make an angle of $-45°$ with x axis of the plate system. The stiffnesses of the composite plate are‡

$$A_{11} = A_{22} = 1.021 \times 10^6 \text{ lb/in.}; \; A_{12} = 0.850 \times 10^6 \text{ lb/in.}$$

$$A_{16} = A_{26} = 0; \; A_{66} = 0.862 \times 10^6 \text{ lb/in.}$$

$$B_{11} = B_{12} = B_{22} = B_{66} = 0; \; B_{16} = B_{26} = 1.99 \times 10^4 \text{ lb-in/in.}$$

$$D_{11} = D_{22} = 1.011 \times 10^3 \text{ in.-lb}; \; D_{12} = 0.842 \times 10^3 \text{ in.-lb}$$

$$D_{16} = D_{26} = 0; \; D_{66} = 0.854 \times 10^3 \text{ in.-lb}$$

The 11-in. × 9.75-in. plate is simply supported on all four sides and is subjected to a compressive load $\bar{N}_x$ lb/in. along the edge $x = \pm A$. Since the coupling terms B_{16} and B_{26} are active, symmetry is absent and the plate was modeled using 16 nonlinear face elements, each 2.75 in. × 2.4375 in. Using the same procedure as in the previous problem, a curve of center deflection vs applied load was plotted and is shown in Fig. 7.

The buckling load predicted is $\bar{N}_{CR} = 368$ lb/in. The average value of two tests reported in Ref. 12 give the experimental buckling load to be 370.5 lb/in. Neglecting the coupling stiffnesses, classical orthotropic plate theory predicts a buckling load of 745 lb/in., more than double the experimental values. From the results it is clear that the effects of the coupling stiffnesses cannot be neglected and that the discrete element method reported should be a valuable analysis tool for composite-type structures.

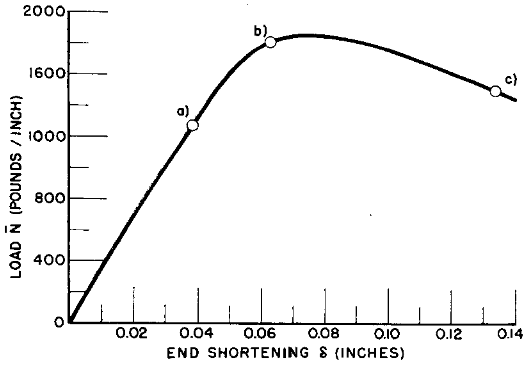

Fig. 8 Sandwich panel (load vs end shortening).

‡ For details concerning fiber content, method of calculating stiffnesses etc., see Ref. 12, plate 409a.

Compressed Sandwich Cylindrical Shell Panel

A sandwich cylindrical shell panel of radius $R_c = 100$ in. is subjected to end-shortening in the longitudinal direction. The geometric and elastic properties of the faces and core are the same as those for the compressed sandwich plate discussed previously (Fig. 5), but the boundary conditions are significantly different. All the edges of the panel are supported to prevent radial displacement and they are assumed to remain straight. The longitudinal edges are prevented from displacing in the circumferential direction by constraining the panel between "walls." The imposed boundary conditions are:§

$$u_f(-A,y) = \delta_f, \; u_f(+A,y) = -\delta_f$$

$$v_f(\pm A,y) = v_f(x,\pm B) = 0, \; f = 1,2$$

$$w(\pm A,y) = w(x,\pm B) = 0$$

A uniform shortening of the circumferential boundaries is imposed on both faces of the sandwich (i.e., $\delta_1 = \delta_2 = \delta$) by "rigid blocks." The equivalent uniform load required to maintain the displacement pattern induced by the imposed end-shortening is calculated from the following expression:

$$\bar{N} = \bar{N}_{1x} + \bar{N}_{2x} = \sum_{f=1}^{2} \frac{Et_f}{B_f(1-\nu^2)} \int_0^{B_f} (\epsilon_{fx} + \nu\epsilon_{fy})|_{x=-A} dy$$

Assuming doubly symmetric behavior, the panel was modeled using four nonlinear sandwich cylindrical shell elements. Satisfying geometric admissibility, requiring membrane strain continuity in the faces, and taking the imposed displacement boundary condition into account reduces the problem to the minimization of a function of 88 variables.

A plot of the equivalent uniform end load $\bar{N}$ vs end-shortening δ is given in Fig. 8. In Fig. 9 the transverse deflections of selected points on the panel are plotted versus load level $\bar{N}$. In Fig. 10, three distinct transverse displacement patterns (a, b, and c) that correspond to different stages in the end shortening process (see points a, b, and c in Fig. 8) are exhibited. It

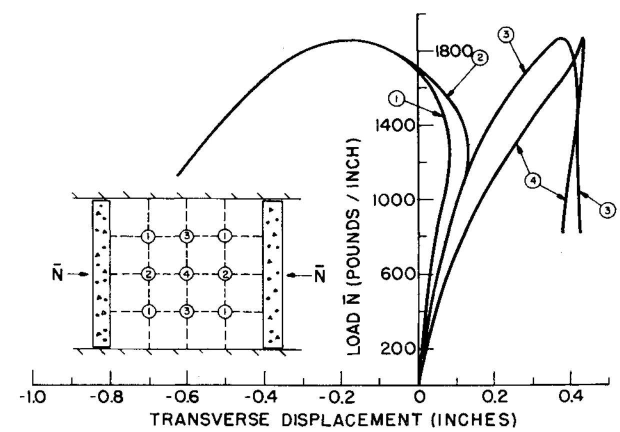

Fig. 9 Compressed sandwich panel.

§ In order to facilitate the discussion of the boundary conditions, the thickness of the core is temporarily neglected (i.e., it is assumed that $R_f = R_t = 100$ in.); however, the numerical results presented do account for the core thickness.

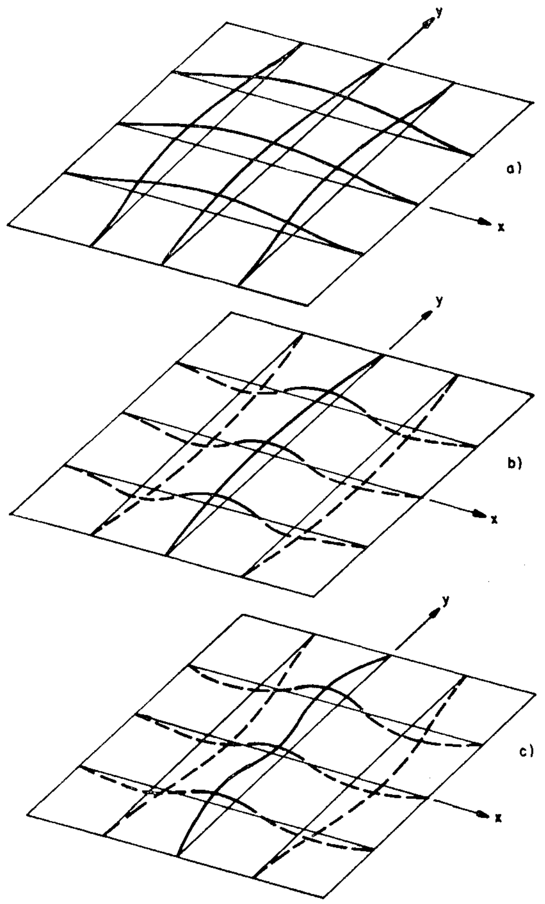

Fig. 10 Displacement configurations for sandwich panel.

should be emphasized that the results for this example are based on the assumption of doubly symmetric behavior.

Conclusions

The discrete element method has been applied to the finite deflection analysis of sandwich plates and cylindrical shells with unbalanced laminated faces. The geometric nonlinearity was incorporated in the analysis by using a set of finite-displacement, strain-displacement equations. The particular set of strain-displacement equations used limits the method to cases where the rotations of the deformed geometry relative to the undeformed geometry are small (i.e., $\sin\theta \backsimeq \theta$, $\cos\theta \backsimeq 1$). The formulation presented was restricted to linear elastic material behavior; however, the approach can be extended to any material behavior law that can be represented by a strain energy density-type of potential function. Although the method was applied to sandwich and laminated structures which can be adequately modeled using rectangular elements, the method can be extended to parallelogramic element using skew coordinates.[15]

The displacement behavior was described in terms of the membrane displacements of the individual faces and the transverse displacement of the sandwich system. In this way transverse shear deformation in the core are accounted for and a rather wide choice of boundary conditions is made available. The analysis of thin anisotropic and transversely heterogeneous laminated plates and cylindrical shells can be dealt with as a specialization by considering only one face of the sandwich. It should also be noted that by representing the potential energy in terms of the various stiffnesses of the faces and core, the method is not bound to any one of the several micromechanics theories available for laminated structures.

The displacement variables were approximated using bicubic Hermite interpolation polynomials and undetermined nodal coefficients. This type of approximation makes it possible to readily satisfy the geometric admissibility conditions and therefore guarantees conforming solutions. Also, the reference surface strains on the faces can be made continuous between elements so that accurate stress predictions should result for typical thin face sandwich systems. The method also lends itself to structural idealizations involving elements joined at arbitrary angles.

The numerical examples given are intended to illustrate the potential of the method presented for the finite deflection and postbuckling analysis of sandwich and laminated structures. Solutions were obtained by searching for the local minimum of the discretized total potential energy. A conjugate gradient algorithm, which incorporates a variable scaling transformation, was used to carry out the minimization, and it was found to be effective. Typical solution times for a single point on the load versus end shortening curve in Fig. 8 was less than one minute on the Univac 1108 computer using the Fortran IV program. It is noted that the method does not have to be used in an incremental mode; however the determination of a series of points for a load-displacement type curve, such as that shown in Fig. 8, is most efficiently obtained by incrementation.

References

[1] Reissner, E., "Finite Deflection of Sandwich Plates," *Journal of the Aerospace Sciences*, Vol. 15, 1948, pp. 435–440.

[2] Bogner, F. K. et al., "Development and Evaluation of Energy Search Methods of Nonlinear Structural Analysis," TR-65-113, 1965, Air Force Flight Dynamics Lab., Wright-Patterson Air Force Base, Ohio.

[3] Schmit, L. A., Bogner, F. K., and Fox, R. L., "Finite Deflection Structural Analysis Using Plate and Shell Discrete Elements," *AIAA Journal*, Vol. 6, No. 5, May 1968, pp. 781–791.

[4] Bogner, F. K., "Finite Deflection Discrete Element Analysis of Shells," TR-67-185, June 1968, Air Force Flight Dynamics Lab., Wright-Patterson Air Force Base, Ohio.

[5] Dong, S. B. et al., "Analysis of Structural Laminates," ARL 76, Sept. 1961, Aeronautical Research Lab., Office of Aerospace Research, Wright-Patterson Air Force Base, Ohio.

[6] Bogner, F. K., Fox, R. L., and Schmit, L. A., "The Generation of Interelement-Compatible Stiffness and Mass Matrices by the Use of Interpolation Formula," *Proceedings of the Conference on Matrix Methods in Structural Mechanics*, TR-66-80, 1966, Air Force Flight Dynamics Lab., Wright-Patterson Air Force Base, Ohio.

[7] Monforton, G. R. and Schmit, L. A., "Finite Element Analysis of Sandwich Plates and Cylindrical Shells with Laminated Faces," *Proceedings of the Conference on Matrix Methods in Structural Mechanics*, TR-68-150, 1968, Air Force Flight Dynamics Lab., Wright-Patterson Air Force Base, Ohio.

[8] Fletcher, R. and Reeves, C. M., "Function Minimization by Conjugate Gradients," *The Computer Journal*, Vol. 7, 1964, pp. 163–168.

[9] Fox, R. L. and Stanton, E. L., "Developments in Structural Analysis by Direct Energy Minimization," *AIAA Journal*, Vol. 6, No. 6, June 1968, pp. 1036–1042.

[10] Kan, H. P. and Huang, J. C., "Large Deflection of Rectangular Sandwich Plates," *AIAA Journal*, Vol. 5, No. 9, Sept. 1967, pp. 1706–1708.

[11] Plantema, F. J., *Sandwich Construction*, Wiley, New York, 1966.

[12] Mandell, J., "An Experimental Study of the Buckling of Anisotropic Plates," M.Sc. thesis, 1968, Solid Mechanics, Structures and Mechanical Design Division, Case Western Reserve University, Cleveland, Ohio.

[13] Roorda, J., "Some Thoughts on the Southwell Plot," *Journal of the Engineering Mechanics Division, ASCE*, Vol. 93, No. EM6, 1967, pp. 37–48.

[14] Lekhnitski, S. G., "Anisotropic Plates," *Contributions to the Metallurgy of Steel*, No. 50, American Iron and Steel Institute, 1956.

[15] Monforton, G. R. and Schmit, L. A., "Finite Element Analysis of Skew Plates in Bending," *AIAA Journal*, Vol. 6, No. 6, June 1968, pp. 1150–1152.